# Atomic force microscopic study of the structure of high-density polyethylene deformed in liquid medium by crazing mechanism

D.V. BAGROV, A.Y. YARYSHEVA, E.G. RUKHLYA, L.M. YARYSHEVA, A.L. VOLYNSKII & N.F. BAKEEV

*Faculty of Chemistry, M. V. Lomonosov Moscow State University, Moscow, Russia*

## Summary

A procedure has been developed for the direct atomic force microscopic (AFM) examination of the native structure of high-density polyethylene (HDPE) deformed in an adsorption-active liquid medium (AALM) by the crazing mechanism. The AFM investigation has been carried out in the presence of a liquid medium under conditions preventing deformed films from shrinkage. Deformation of HDPE in AALM has been shown to proceed through the delocalized crazing mechanism and result in the development of a fibrillar-porous structure. The structural parameters of the crazed polymer have been determined. The obtained AFM images demonstrate a nanosized nonuniformity of the deformation and enable one to observe the structural rearrangements that take place in the deformed polymer after removal of the liquid medium and stress relaxation. A structural similarity has been revealed between HDPE deformed in the AALM and hard elastic polymers.

## Introduction

Crazing is one of the types of plastic inelastic deformation of polymers. This type of deformation is distinguished by the development of a fibrillar-porous structure formed by oriented polymer fibrils with a diameter of 5–20 nm separated by microvoids of nearly the same sizes (Kambour, 1973; Kausch & Argon, 1990). Stretching of polymers in physically active liquid media (hydrocarbons, oils, alcohols, surfactants, etc.) is known to promote the development of deformation by the crazing mechanism and to accelerate their breakage (Altstädt, 2005; Robeson, 2013).

Since polymer breakage is preceded by nucleation of crazes and cracks, the service properties of polymers are estimated based on the monitoring of their appearance upon the complex action of an ambient liquid and stress. In the literature, this phenomenon is referred to as environmental stress cracking/crazing, and the studies in this field are focused on the suppression or deceleration of the development of crazes and cracks with the aim to enhance the resistance of polymers to environmental effects (Cornélis & Kander, 1996; Lagaron *et al.*, 1999; Plummer *et al.*, 2001; De Focatiis & Buckley, 2008).

At the same time, the development of crazes upon polymer deformation in an adsorption-active liquid medium (AALM) may appear to be a positive factor, because the deformation is accompanied by the development of a finely disperse fibrillar-porous structure on the nanosized level (Kambour, 1973; Kramer, 1979; Volynskii & Bakeev, 1995). In Volynskii & Bakeev (1995), Volynskii *et al.* (2000) and Arzhakova *et al.* (2011) conditions were found under which the deformation of amorphous glassy and crystalline polymers in liquid media occurs through the crazing mechanism and gives rise to the formation of nanoporous materials with a porosity as high as 40–60%. It is of particular interest that polymer deformation in solutions of various low- or high-molecular-mass compounds is accompanied by their penetration into the nanoporous structure of crazes to result in the formation of nanocomposites and highly dispersed polymer–polymer blends (Trofimchuk & Yablokova, 2001; Trofimchuk *et al.*, 2005a, b, 2007; Rukhlya *et al.*, 2011; Gruzd *et al.*, 2013).

Thus, the investigation of polymer crazing in liquid media is an urgent problem from the viewpoints of both the determination of the influence of liquid media on the mechanism of polymer deformation and the creation of highly disperse fibrillar-porous structures in films and fibres, as well as the production of nanocomposites and polymer–polymer blends on their basis.

The use of AALMs enlarges the assortment of polymers deformed by the crazing mechanism. This phenomenon has most comprehensively been studied for the deformation of amorphous glassy polymers. Stretching of glassy polymers causes crazing that is commonly referred to as the classical crazing. This process has been described in detail elsewhere (Volynskii & Bakeev, 1995). Here we only note that the
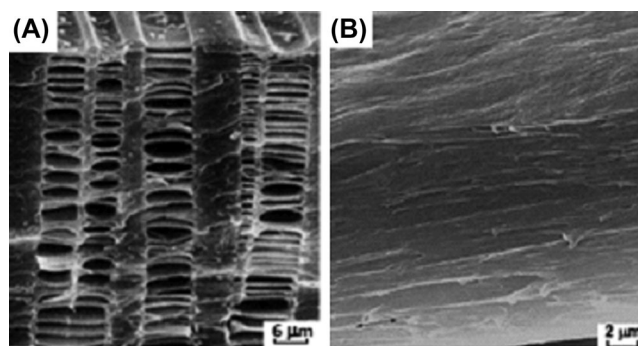
**Fig. 1.** Scanning electron micrographs taken from cleavages of (A) poly(ethylene terephthalate) deformed by 100% in a AALM (Volynskii & Bakeev, 1995) and (B) HDPE stretched by 200% in the same medium (at these strains, equal volume porosities developed in the polymers; in both cases, the medium was removed under isometric conditions, and the micrographs were taken after the shrinkage of the samples).

structure of crazes that develop in AALMs is very labile and unstable; therefore, the removal of an AALM from crazes is accompanied by profound structural rearrangements. In this context, the so-called native structure that is formed immediately after the deformation, when the polymer still contains the AALM as a stabilizer, and the structure that results from the drying and shrinkage of the deformed polymer are distinguished between. The native structure of crazes cannot be investigated with an electron microscope, because this method implies evacuation of an object under examination. Therefore, the structure of native crazes was so far studied using small-angle X-ray scattering (SAXS) (Yefimov *et al.*, 1990) and liquid permeability under pressure gradients (Yarysheva *et al.*, 1989). However, the interpretation of experimental data obtained by these methods requires the use of model concepts, thus leading to ambiguous results.

Note that the classical crazing of polymers in liquid media is not the only type of deformation that is accompanied by the development of porosity. Depending on a polymer structure, nature of a medium and stretching conditions, crystalline polymers can be deformed by two mechanisms, i.e. the classical mechanism that is similar to the crazing of glassy polymers and the delocalized mechanism that is inherent in crystalline polymers alone (Volynskii & Bakeev, 1995; Sinevich *et al.*, 1998; Volynskii *et al.*, 2000). The main difference between the two kinds of crazing consists in the sizes of the local zones of deformation.

Figure 1 illustrates scanning electron microscopic (SEM) images that characterize the structure of polymers deformed in an AALM by the crazing mechanism and dried under isometric conditions (Volynskii & Bakeev, 1995). In the case of the classical crazing, the method of electron microscopy enables one to observe individual crazes and the regions of an undeformed polymer between them (Fig. 1A). The width of crazes may be as large as several dozen micrometres, while their length may

be still larger, i.e. several millimetres and above. The internal structure of the crazes is composed of fibrils, which connect opposite walls of crazes, and voids between the fibrils.

When deforming crystalline polymers in AALMs, individual crazes fail to be observed by these methods (Fig. 1B), although the porosity develops simultaneously and uniformly throughout the bulk of a polymer being deformed. Despite the fact that crazing of this kind has been comprehensively investigated, direct data on the morphology of the resulting porosity are unavailable. This is primarily due to the fact that AALM removal from the pores and stress relaxation are accompanied by shrinkage or collapse (healing) of the porous structure. When a polymer is deformed by the classical crazing mechanism, the presence of large zones of a bulk material greatly hinders the shrinkage upon the stress relaxation, and this circumstance makes it possible to observe the structure of crazes in contrast to a polymer that has been deformed through the delocalized crazing mechanism. Thus, in order to characterize the structure of a crystalline polymer deformed in an AALM by the crazing mechanism, samples should be examined under load and in the presence of a liquid that cannot be done by the traditional methods of transmission or SEM.

A great advance has been achieved in the study of the structure and properties of various materials on the submicron level after the methods of scanning probe microscopy and, in particular, atomic force microscopy (AFM) were developed and began to be applied (Magonov & Yerina, 2005). The continuous improvement of different modes of AFM and procedures of sample preparation widens the scope of application of this method in different fields of research, such as colloid and surface science, materials engineering and biology (Magonov & Reneker, 1997; Cappella & Dietler, 1999; Hodges, 2002; Butt *et al.*, 2005). Although AFM can access only the surface structure and not the bulk structure, the advantage of AFM is the ability to study polymer crystallization, melting and deformation *in situ*.

This work is devoted to the study of the structural transformations that take place in crystalline polymers being deformed. In most cases, the literature data on the evolution of the structure of crystalline polymers being stretched in air deal with the investigation of thin films by transmission electron microscopy (TEM) or the study of block samples by SEM carried out *ex situ* and do not separate the relaxation process and deformation (Petermann *et al.*, 1982; Yang & Thomas, 1984; Adams *et al.*, 1986; Butler & Donald, 1997). In contrast to electron microscopy, AFM allows one to perform high-resolution monitoring of objects immediately in the process of their stretching.

Hild *et al.* (1996) were the first to use AFM for *in situ* visualizing the structure of a crystalline polymer stretched with a homebuilt stretching device. Hard elastic polypropylene, which is distinguished by a highly ordered structure of lamellae-oriented normal to the extrusion axis, was selected for the study. The sizes of the crystalline rows and the

noncrystalline interlayers of unstretched and stretched polymers were determined and the data obtained were analysed in accordance with the available models of hard elastic polymers and mechanisms of porous structure formation in them. Further, different types of stretching devices were developed and their suitability for the investigation of deformation-induced surface changes in crystalline polymers was demonstrated (Hild *et al.*, 1998; Bamberg *et al.*, 2006).

The analysis of the deformation mechanism of crystalline polymers by *in situ* AFM consists not only in taking micrographs, but also in studying film roughening as a result of stretching. As has been shown in (Opdahl & Somorjai, 2001), the deformation of low- (LDPE) and high-density polyethylene (HDPE) increases the polymer roughness. The surface-roughening effect is completely reversible upon stretching in the elastic regime and partially reversible for stretching in the plastic regime.

The data obtained on the evolution of the structure of nylon-6-rubber blends with the help of AFM and a mini stretching device during the stretching and relaxation processes have been reported in Oderkerk *et al.* (2002). During stretching, the plastic deformation is initiated in the zones where the nylon matrix between the rubber particles is thinnest. When the external force is eliminated, dispersed rubber phase pulls back the plastically deformed nylon moieties by either buckling or bending.

The structures of HDPE and linear low-density polyethylene (LLDPE) films have been investigated during both deformation and relaxation processes (Li *et al.*, 2003). After the stress relaxation, substantial structural changes have been observed for samples occurring in the free state.

In Thomas *et al.* (2007, 2009) *in situ* AFM was employed to gain a deeper insight into the nucleation, development and coalescence of crazes in poly(1-butene) being stretched, and the advantage of this method over TEM for thin films was demonstrated. Crazes were primarily nucleated in the equatorial region of spherulites. The authors assumed that crazes were formed by the instable meniscus mechanism similarly to that observed for the crazing of glassy polymers. These data were obtained for poly(1-butene) with spherulite sizes of 20–100 $\mu$m, whereas, upon the deformation of spherulites with sizes of 20 and 5 $\mu$m, the shape of the deformed spherulites remained actually elliptical up to the rupture without clues of fibrillar transformation.

The evolution of the spherulitic structure in the preyield strain range under tensile testing was investigated by *in situ* AFM for three semicrystalline polymers, namely, polycaprolactone, poly(1-butene) and polyamide 6 (Detrez *et al.*, 2010, 2011). These materials have different spherulite sizes, crystallinity indices, lamella thicknesses and glass transition temperatures of the amorphous phase. AFM revealed that fragmentation of the crystalline lamellae occurred well before the yield strain, beginning in the vicinity of the core region of the spherulites and extending towards the periphery, for all

polymers. This was claimed to be an evidence that lamella fragmentation was a basic mechanism of breakage without significant cavitation of these polymers at low strains.

Thus, the aforementioned examples demonstrate that *in situ* AFM makes it possible to study in detail the evolution of the structure of crystalline polymers being stretched in air and judge the mechanism of their deformation.

The study of the native structure and the deformation mechanism of crystalline polymers upon stretching in liquid media is a more complex problem, and, up to the present, direct methods for such researches were unavailable, because they must be carried out for loaded samples in the presence of a liquid. At the same time, AFM is known to be an instrument for performing structural investigations with a high resolution not only in air, but also in liquid media (Magonov & Yerina, 2005; Yarysheva *et al.*, 2011). Therefore, in this work we intend to employ AFM for studying the native structure of polymers deformed in liquid media by the crazing mechanism. By the example of HDPE deformed in an AALM, it will be shown that AFM enables one to visualize the fibrillar-porous structures of crazed polymers and estimate the parameters thereof.

## Experimental

### Materials

The objects for the study were HDPE ($M_w = 210\ 000$ and $M_n = 7000$ g mol$^{-1}$) films 25 $\mu$m thick (Stamylan, DSM) produced by blown extrusion. Films with sizes of $40 \times 20$ mm were stretched in a water–ethanol solution (1:7, vol/vol) at room temperature and a rate of 5.4 mm min$^{-1}$ in the direction coinciding with the extrusion axis.

### Differential scanning calorimetry (DSC) experiments

The experiments were performed using a TA 4000 thermo-analyzer (Metter). The mass of an examined sample was 1.5 mg. Ideal crystal melting heat, which was used to calculate the degree of crystallinity, was 293 J g$^{-1}$. The heating rate was 10 K min$^{-1}$. Lamella thickness was calculated by the following formula:

$$L_c = L_{saxs}(d/d_c) \times K_c, \quad (1)$$

where $L_{saxs}$ is the long period determined by SAXS (25 nm), $d$ and $d_c$ are the densities of the polymer and its crystalline phase (0.960 and 1.003), respectively and $K_c$ is the degree of crystallinity (59%) determined from the DSC data.

### X-ray diffraction analysis

SAXS measurements were carried out with a Nanostar instrument (Bruker AXS) equipped with a CuK$_\alpha$ generator of X-rays ($\lambda = 0.154$ nm).

*Porosity*

Porosity (*W*) of the deformed polymer was calculated from changes in the geometric sizes of the films as the ratio of volume increment ($\Delta V$) resulting from film stretching to initial sample volume ($V_0$), $W = (\Delta V / V_0) \times 100$ (%).

*Film shrinkage*

Film shrinkage was determined as $\lambda = (L_{def} - L_{shr}) / (L_{def} - L_0)$, where $L_0$ is the initial sample length, $L_{def}$ is the length of a sample after deformation and $L_{shr}$ is the sample length after shrinkage.

*SEM*

Structure of the poly(ethylene terephthalate) and the HDPE samples was studied by a scanning electron microscope (Hitachi S-520, Japan). Prior to the SEM observations, the samples were fractured in the liquid nitrogen along to the direction of tensile drawing. The fractured surfaces were decorated with gold on an Eiko IB-3 unit by the method of ionic plasma sputtering.

*AFM experiments*

All AFM experiments were carried out using a Solver Pro-M atomic force microscope (NT-MDT, Zelenograd, Russia) in the ≪scanning by probe≫ configuration. A Smena scanning head equipped with closed-loop feedback sensors was applied (scanner range of $100 \times 100 \times 7$ $\mu$m).

The scanning was carried out in the contact and tapping modes in air and liquid. When scanning in air, an NSG10 (NT-MDT) and an MSCT-AUHW (Bruker, former Veeco, Santa Barbara, CA, USA) cantilevers were applied in the tapping and contact modes, respectively. The scanning in the liquid was performed using MSCT-AUHW cantilevers (Bruker) in both contact and tapping modes. Neither in air nor in liquid, an essential difference was observed between the height images obtained in the contact and tapping modes. However, when scanning in air, we preferred the tapping mode to record the phase contrast images simultaneously with the height images, which is less inefficient in a liquid because of a rather low cantilever quality factor.

The AFM images were processed using the Femtoscan online software package (Advanced Technologies Center, Russia). Each scan was processed using ≪Fit Lines≫ and ≪Plane Fit≫ functions to avoid the shift of rows and the general slope, respectively. When necessary, the noise was reduced by median filtering or averaging. In some cases, the macroscopic height variations were removed using the spline filtering. When plotting and analysing the sections, each section profile was constructed by averaging the profiles over three adjacent section lines.

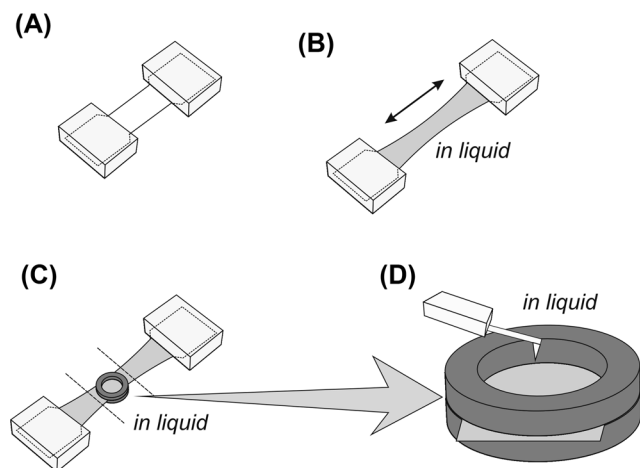*Procedure for investigating the structure of HDPE deformed in the medium*

The AFM monitoring of variations in the structure of polymers being stretched is commonly performed using a microscope, which implements scanning by a cantilever that has actually no limitations on sample sizes and masses and can be mounted on a tensile-testing machine. Using this combined system that comprises an AFM and a stretching unit, the experiment is commonly performed as follows: a film is stretched under a stepwise increasing load, and an image of a selected surface region is obtained at each tensile strain. The stretching is commonly controlled with an optical system to retain the cantilever over the same sample region throughout the experiment. Such combined systems were employed to study, e.g. the stretching of polypropylene films (Kraev *et al.*, 2007) and crazing of poly(1-butene) by stretching in air (Thomas *et al.*, 2009).

The application of these systems for studying polymers being deformed in liquid media is extremely complicated, because, for this purpose, it is necessary to place the mobile clamps of a tensile-testing machine into a vessel and to bring a cantilever to contact with a sample in a liquid. In this work, the native structure of HDPE was studied in the following way. Initially, a sample was stretched to some tensile strain with a stretching unit operating in the liquid medium. Then, without removing the sample from the liquid medium and the clamps of the stretching unit, it was fastened to a circular frame to fix its sizes throughout the perimeter and prevent it from shrinkage. The frame with the sample was placed into a Petri dish filled with the medium (water–ethanol solution) in which the stretching had been implemented. A support was mounted under the centre of the film to reduce vibration. The preparation of a sample for the AFM examination is schematically represented in Figure 2. This system enabled us to carry out the AFM examination of the deformed film surface in the presence of the liquid under the conditions that prevented the samples from shrinkage; that is, to study, namely, the native structure thereof.

**Results and discussion**

*Structure of initial HDPE films*

The deformation mechanism of crystalline polymers strongly depends on the structure of an initial polymer (Volynskii *et al.*, 2000). According to the DSC data, the degree of crystallinity of the HDPE films under investigation was 59%. The films had been produced by blown extrusion; that is, under the conditions of stressed polymer crystallization. In the literature, the structures formed under these conditions are referred to as row-nucleated crystalline structures or the Keller–Machin structures (Keller & Machin, 1967). In the course of blown extrusion, polymers crystallize under the effect of stresses
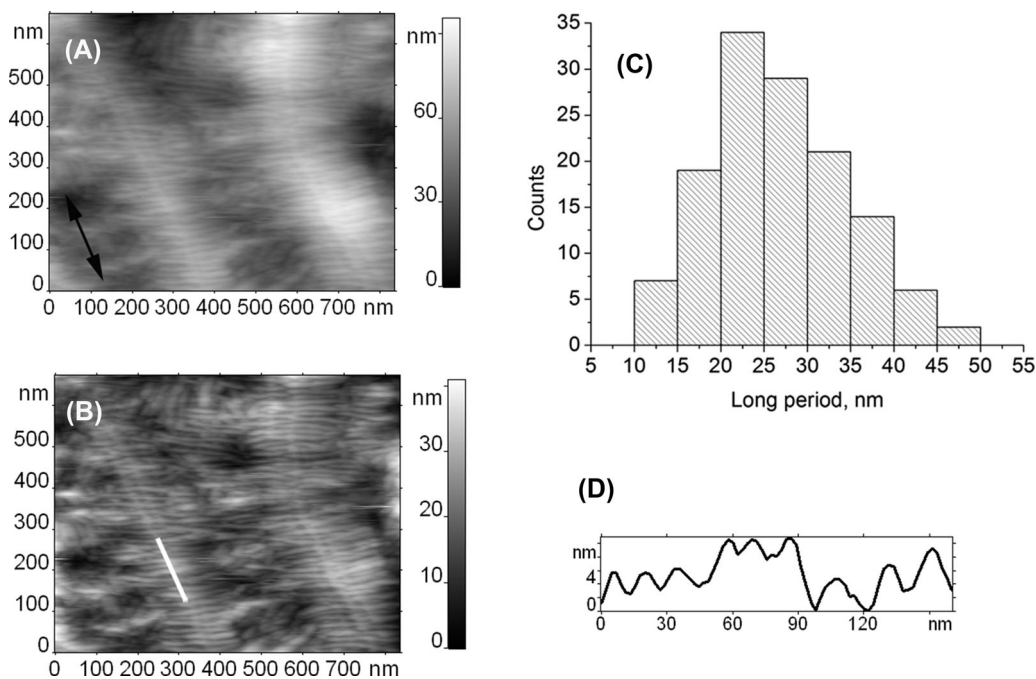
lae are assembled into columns oriented along the stretching axis. These formations are typical for polymers with a row structure and were previously observed for HDPE films produced by blown extrusion (Zhang *et al.*, 2004). The image can be improved by spline filtering (Fig. 3B), which eliminates the large height variations corresponding to columns. Figure 3(D) demonstrates the height profile along the line parallel to the extrusion axis. The asperities in the height image correspond to lamellae, although the distance between the two adjacent maxima is the long period in the polymer structure. According to the distribution histogram (Fig. 3C), the long period covers the range 10–50 nm, and its mean value is $27 \pm 8$ nm. If the film is examined in air, AFM provides a $35 \pm 7$ nm long period value (images not shown). This difference may be explained by the influence of the capillary force, which increases the tip-sample interaction. Similar effects were observed in Wawkuschewski *et al.* (1993). It should be noted that the image of initial HDPE in the liquid medium is more detailed and qualitative.

X-ray diffraction analysis is known to be a common method for studying the structure of crystalline polymers. The SAXS pattern of HDPE is presented in Figure 4. Intense drop-shaped reflections are seen at the meridian and less intense ones are observed at the equator, thus indicating an anisotropic distribution of the scattered intensity relative to the texture axis. This SAXS patterns, which is inherent in extruded HDPE films, indicates the presence of a lamellar structure, with lamellae being mostly oriented perpendicularly to the extrusion axis



**Fig. 2.** Scheme of sample preparation: (A) initial sample fixed in the clamps, (B) sample stretching in the AALM (stretching direction is denoted by the arrow), (C) deformed sample fastening to the circular frame and (D) AFM examination.

directed along and normal to the extrusion axis; therefore, lamellae may have different orientations in resulting polymers depending on the moulding conditions (Kojima *et al.*, 1997; Lu *et al.*, 2001; Prasad *et al.*, 2001; Godshall *et al.*, 2003; Zhang *et al.*, 2004; Ajji *et al.*, 2005).

Figure 3 shows the AFM height (A, B) images of the initial (nondeformed) HDPE obtained in liquid medium. The lamel-



**Fig. 3.** AFM images of initial HDPE film structure: (A) height image, (B) height image after spline filtering, (C) histogram of long-period distribution, (D) relief sections along lines in the direction of the extrusion axis. The direction of extrusion in the course of film production is denoted in panel (A) by the arrow.
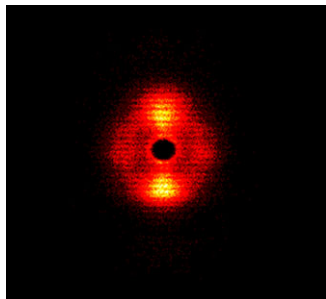
**Fig. 4.** SAXS pattern of initial HDPE.

(Godshall *et al.*, 2003). For reflections located at the meridian $2\theta = 0.35$, the long period appeared to be 25 nm, which is in good agreement with the value obtained by AFM. AFM provides information only about the surface structure, whereas SAXS examines the bulk sample. The good agreement of the obtained values confirms the data correctness.

Thus, initial HDPE films have a lamellar structure, with lamellae being predominantly oriented perpendicularly to the extrusion axis. Subsequent HDPE stretching was carried out along the extrusion axis of the initial films.

*AFM study of the structure of HDPE deformed by the crazing mechanism*

As was shown in Yefimov *et al.* (1988), Arzhakova *et al.* (2011) and Yarysheva *et al.* (2012), deformation of HDPE in AALMs, such as aliphatic alcohols or hydrocarbons, proceeds through the crazing mechanism and is accompanied by the development of porosity. In this work, HDPE was stretched in a water–ethanol solution. The porosity determined from a change in the volume of a sample stretched in the medium by 200% was about 60%.

The AFM height image of HDPE stretched by 200% in the water–ethanol solution and the same image subjected to the spline filtering for levelling the relief are depicted in Figures 5(A) and (B), respectively. Similarly to the case of initial HDPE, these images show columns directed along the extrusion axis and composed of lamellae oriented perpendicularly to the extrusion axis. At the same time, the images demonstrate notable changes in the structure of the stretched polymer, as compared with that of the initial film (Fig. 3). It can be seen that the stretching gives rise to the formation of crazes, i.e. particular zones of deformed polymer, which have a fibrillar-porous structure. Fibrils are oriented along the stretching axis. Lamellae form the craze walls between which fibrils are located.

The values corresponding to long period $L$, i.e. the sums of the lamella thickness and the fibril length, were determined from the section profiles oriented along the stretching axis (line 1 in Fig. 5B). As can be seen from the histogram (Fig. 5E), these values vary in a wide range of 25–300 nm. Lamella thickness determined from the same section profiles appeared to be

15–20 nm, which is in good agreement with the value (14 nm) calculated from the SAXS and DSC data by Eq. (1) presented in the 'Experimental' section.

Distances $l$ between adjacent maxima, which correspond to the sums of fibril and pore diameters, were determined from the section profiles along the line perpendicular to the axis of HDPE stretching (line 2 in Fig. 5B). Unfortunately, this image does not enable us to reliably determine the diameters of fibrils and pores between them separately, because their values are comparable with the cantilever curvature radius ($\sim$10 nm). However, distance $l$ between the tops of fibrils, which is determined as the distance between the maxima in the section profiles, is independent of the cantilever curvature radius. This value lies in the range of 15–35 nm and is comparable with the data obtained by the X-ray diffraction analysis and the method of liquid permeability under pressure gradient for fibril diameters and effective pore diameters in crazed polymers (Yefimov *et al.*, 1988; Arzhakova *et al.*, 2011).

Figure 5 presents images that are most typical for HDPE deformed in the liquid medium by the crazing mechanism. However, micrographs that demonstrate regions of nonuniform deformation containing both individual lamellae (Fig. 6A, region 1) and stacks thereof (Fig. 6A, region 2) were taken from the same sample. Moreover, there are regions in which the fibrillar-porous structure of crazes cannot be resolved (Fig. 6B). Possibly, this kind of deformation took place in the microregions of the polymer where the stacks of lamellae are bonded by large amounts of through chains or located at some angle or parallel to the stretching axis rather than perpendicularly to it.

Thus, the AFM data on the structure suggest that the HDPE films are deformed in the water–ethanol solution by the crazing mechanism with the formation of a fibrillar-porous structure.

*AFM study of the structure of HDPE deformed by the crazing mechanism and subjected to medium removal and stress relaxation*

As was mentioned above, the structure of polymers deformed by the crazing mechanism is thermodynamically unstable. The removal of the medium or the stress relaxation cause substantial changes in the structure of a deformed polymer.

Figure 7 shows the AFM image of (A) the native structure of HDPE deformed in water–ethanol solution and (B) the structure of the same sample after the removal of the medium (in both cases, the sample is fastened to the circular frame). It can be seen that, although the general pattern of the structure remains preserved (lamellae with fibrils located between them are seen in both of the figures), the removal of the medium leads to marked changes in the structural parameters. The parameter that represents the sum of diameters of fibrils and pores (as measured along lines perpendicular to the stretching axis) increases from 15–35 nm in the medium to 30–80 nm for the dry sample. The increase of tip-sample interaction force, that takes place when we change the scanning conditions from
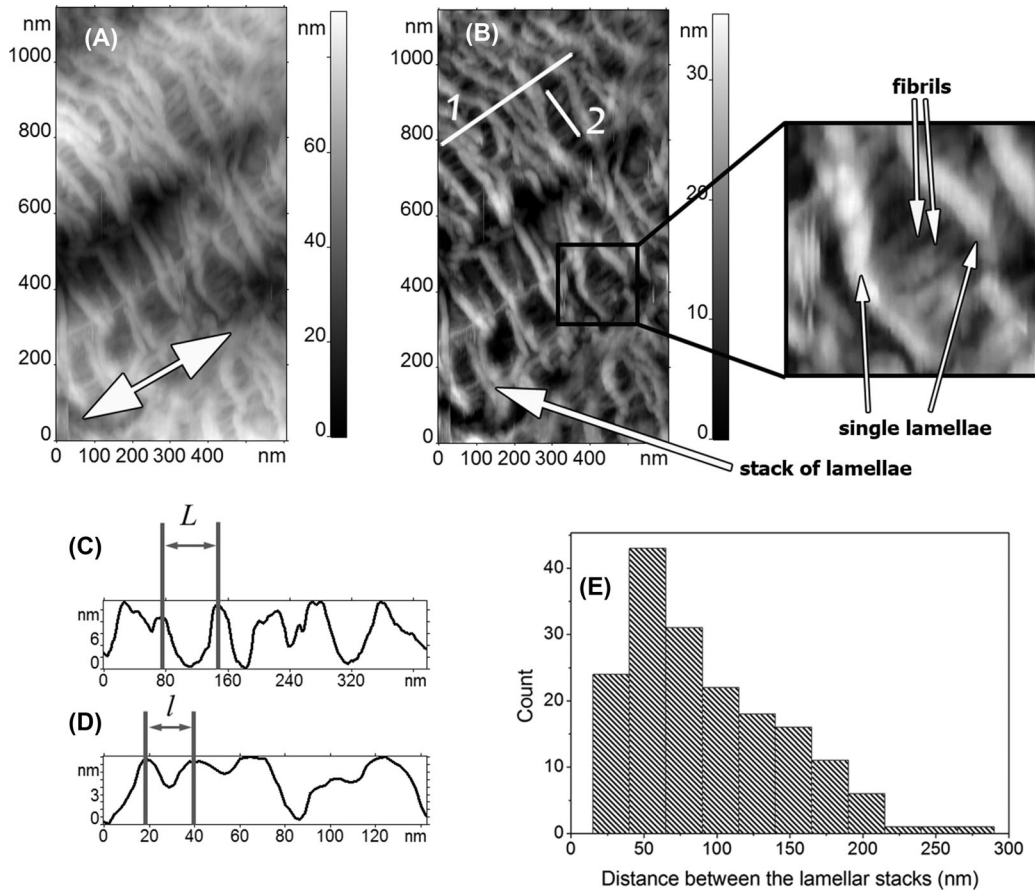
**Fig. 5.** HDPE stretched in water–ethanol solution by 200%. Panel (A): AFM height image; the arrow indicates the stretching direction, which coincides with the extrusion axis; panel (B): AFM height image after spline filtering; panels (C) and (D): relief sections along lines 1 and 2 in panel (B) parallel and perpendicular to the stretching axis, respectively; and panel (E): histogram of long-period distribution.

liquid to air, may also account for the observed increase of the $l$ parameter.

More substantial structural changes are observed for samples without frames, i.e. samples occurring in the free state and subjected to a notable shrinkage (Fig. 7C). For the studied samples stretched by 200%, the shrinkage amounted to about 50%. The fibrillar-porous structure was not observed for such samples. To some extent, this image resembles the structure of initial HDPE (Fig. 3A), but without the previous distinct order in the arrangement of the structural elements. Much attention
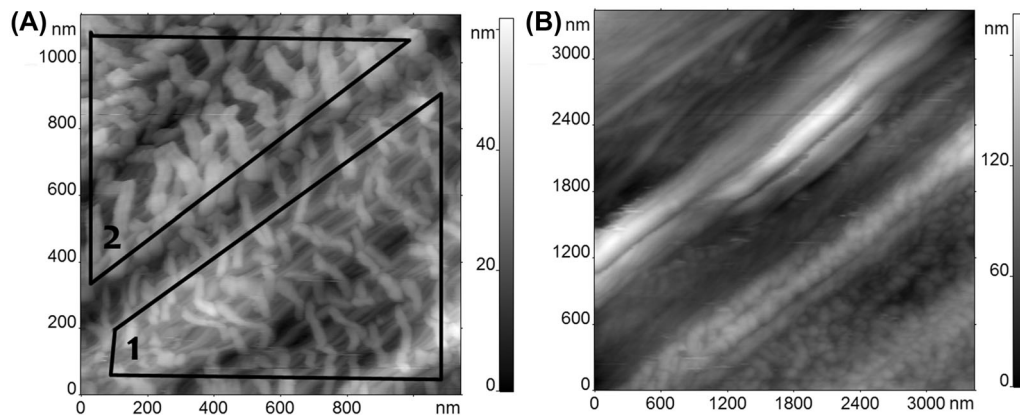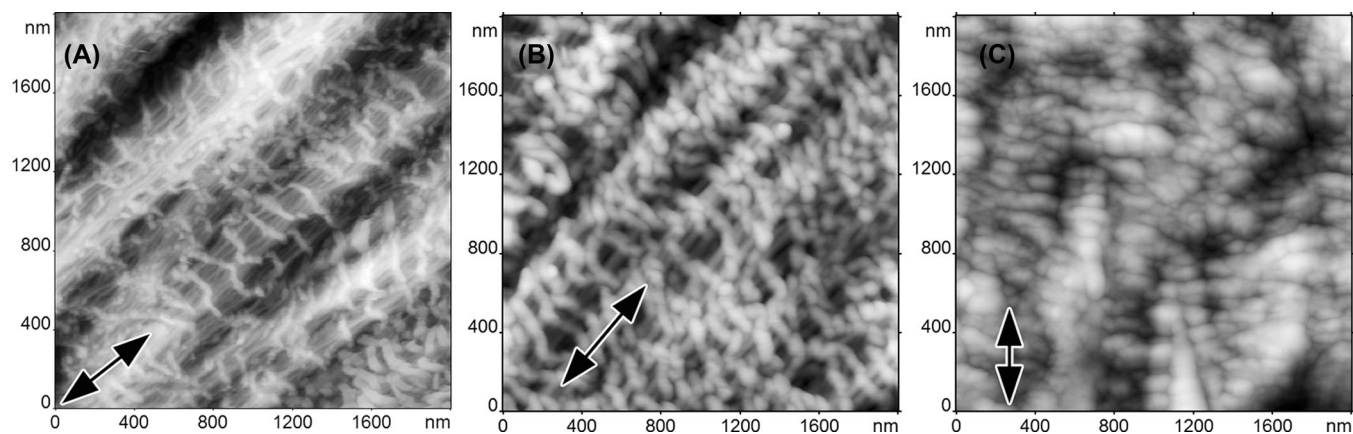


**Fig. 6.** AFM images illustrating the nonuniform structure of HDPE (25 $\mu$m) stretched by 200% in water–ethanol solution.

**Fig. 7.** AFM images of the structure of (A) HDPE deformed by 200% in water–ethanol solution, (B) after the removal of the medium from the sample fastened to the circular frame and (C) after the shrinkage of the deformed sample in the free state in air. The Z-range is 120 nm in (A) and 90 nm in (B) and (C), image contrast was adjusted for clarity. The arrows indicate the stretching direction.

has been paid to the mechanism of the reversible deformation of crazed polymers in the literature (Volynskii & Bakeev, 1995, 2009; Volynskii *et al.*, 2013). In particular, researchers are interested in the question of the extent to which the shrinkage is associated with changes in the entropy and surface energy of a polymer in crazes. Here, we would only like to note the extent to which the native structure of HDPE deformed in the medium may differ from the structure of the polymer after the removal of the medium and the stress relaxation.

**Conclusions**

The AFM method has been used to study the structure of HDPE films produced by blown extrusion. This structure may be considered to be a row-nucleated structure, in which lamellae are mostly oriented normal to the extrusion axis and assembled into columns directed along the extrusion axis.

A procedure has been developed for direct examination of the native structure of a polymer deformed in a liquid medium, which offers ample opportunities for studying polymer crazing. The HDPE deformation in water–ethanol solution has been found to proceed through the delocalized crazing mechanism and be accompanied by the formation of a fibrillar-porous structure. The obtained AFM images indicate a nanosized nonuniformity of deformation and make it possible to estimate changes that take place in a deformed material after the removal of the medium and the stress relaxation.

The data on the native structure of HDPE deformed in AALM have evidently demonstrated the similar and different features of the structures of polymers deformed by the classical (localized) and delocalized crazing mechanisms. The similarity consists in the fact that, in both cases, a fibrillar-porous structure develops in the polymer. However, there are some differences between these two types of crazing. The classical (localized) crazing is mainly observed when amor-

phous glassy polymers are deformed. The development of crazing of this type is associated with an initial imperfection of a material, and individual crazes, as well as regions of an undeformed polymer between them, may be distinguished in a sample. As the deformation develops, the fraction of the nonoriented bulk polymer between crazes continuously diminishes until the entire polymer passes into the oriented state. The nucleation and development of crazes in crystalline polymers are predetermined by their lamellar structure, and the developing fibrillar-porous structure is distributed in the intercrystallite space throughout the sample volume.

The similarity should be noted between the structure of HDPE deformed in a liquid medium and the structure of polymers that are referred to as hard elastics (Sprague, 1973; Cannon *et al.*, 1976; Lee *et al.*, 2006; Volynskii *et al.*, 2013). However, owing to the special procedures of stretching and annealing, the structure of films used as precursors for producing hard elastics is more perfect; therefore, the stretching of these films in air gives rise to the formation of a high-porosity fibrillar-porous structure in them. For HDPE used in this study, the deformation in the air does not lead to the development of the porous structure. The application of liquid media facilitates the deformation by the crazing mechanism (Volynskii & Bakeev, 1995), and such a strict order in the arrangement of lamellae is not required for the development of a high-porosity fibrillar-porous structure in polymers.

## References

Adams, W.W., Yang, D. & Thomas, E. (1986) Direct visualization of microstructural deformation processes in polyethylene. *J. Mater. Sci.* **21**, 2239–2253.

Ajji, A., Zhang, X. & Elkoun, S. (2005) Biaxial orientation in HDPE films: comparison of infrared spectroscopy, X-ray pole figures and birefringence techniques. *Polymer* **46**, 3838–3846.

Altstädt, V. (2005) The influence of molecular variables on fatigue resistance in stress cracking environments. *Intrinsic Molecular Mobility and Toughness of Polymers II* (ed. by H.-H. Kausch). pp. 105–152. Springer, Berlin, Heidelberg.

Arzhakova, O.V., Dolgova, A.A., Yarysheva, L.M., Volynskii, A.L. & Bakeev, N.F. (2011) Development of a stable open-porous structure in the solvent-crazed high-density polyethylene. *Inorg. Mater. Appl. Res.* **2**, 493–498.

Bamberg, E., Grippo, C.P., Wanakamol, P., Slocum, A.H., Boyce, M.C. & Thomas, E.L. (2006) A tensile test device for in situ atomic force microscope mechanical testing. *Prec. Eng.* **30**, 71–84.

Butler, M.F. & Donald, A.M. (1997) Deformation of spherulitic polyethylene thin films. *J. Mater. Sci.* **32**, 3675–3685.

Butt, H.-J., Cappella, B. & Kappl, M. (2005) Force measurements with the atomic force microscope: technique, interpretation and applications. *Surf. Sci. Rep.* **59**, 1–152.

Cannon, S.L., McKenna, G.B. & Statton, W.O. (1976) Hard-elastic fibers. (A review of a novel state for crystalline polymers). *J. Polym. Sci. Macromol. Rev.* **11**, 209–275.

Cappella, B. & Dietler, G. (1999) Force-distance curves by atomic force microscopy. *Surf. Sci. Rep.* **34**, 1–104.

Cornélis, H. & Kander, R.G. (1996) A new method to evaluate solvent stress cracking. *Polym. Eng. Sci.* **36**, 869–878.

De Focatiis, D.S.A. & Buckley, C.P. (2008) Determination of craze initiation stress in very small polymer specimens. *Polym. Test.* **27**, 136–145.

Detrez, F., Cantournet, S. & Séguéla, R. (2010) A constitutive model for semi-crystalline polymer deformation involving lamellar fragmentation. *Comptes Rendus Mécanique* **338**, 681–687.

Detrez, F., Cantournet, S. & Seguela, R. (2011) Plasticity/damage coupling in semi-crystalline polymers prior to yielding: micromechanisms and damage law identification. *Polymer* **52**, 1998–2008.

Godshall, D., Wilkes, G., Krishnaswamy, R.K. & Sukhadia, A.M. (2003) Processing-structure-property investigation of blown HDPE films containing both machine and transverse direction oriented lamellar stacks. *Polymer* **44**, 5397–5406.

Gruzd, A.S., Trofimchuk, E.S., Nikonorova, N.I., Nesterova, E.A., Meshkov, I.B., Gallyamov, M.O. & Khokhlov, A.R. (2013) Novel polyolefin/silicon dioxide/H3PO4 composite membranes with spatially heterogeneous structure for phosphoric acid fuel cell. *Int. J. Hydro. Energy* **38**, 4132–4143.

Hild, S., Gutmannsbauer, W., Lüthi, R., Fuhrmann, J. & Güntherodt, H.J. (1996) A nanoscopic view of structure and deformation of hard elastic polypropylene with scanning force microscopy. *J. Polym. Sci. B Polym. Phys.* **34**, 1953–1959.

Hild, S., Rosa, A. & Marti, O. (1998) Deformation induced changes in surface properties of polymers investigated by scanning force microscopy. *Scanning Probe Microscopy of Polymers* (ed. by B.D. Ratner & V.V. Tsukruk). pp. 110–128. American Chemical Society, Washington, DC.

Hodges, C.S. (2002) Measuring forces with the AFM: polymeric surfaces in liquids. *Adv. Colloid Interface Sci.* **99**, 13–75.

Kambour, R.P. (1973) A review of crazing and fracture in termoplastics. *J. Polym. Sci. Macromol. Rev.* **7**, 1–173.

Kausch, H.H. & Argon, A.S. (1990) *Crazing in Polymers: vol. 2.* Springer-Verlag, Berlin; New York.

Keller, A. & Machin, M.J. (1967) Oriented crystallization in polymers. *J. Macromol. Sci. B* **1**, 41–91.

Kojima, M., Magill, J.H., Lin, J.S. & Magonov, S.N. (1997) Structure and morphology of biaxially oriented films of polyethylenes. *Chem. Mater.* **9**, 1145–1153.

Kraev, A.V., Saunin, S.A., Alekseev, M.E., Safonov, V.A. & Talrose, R.V. (2007) A temperature-deformation unit for scanning electron probe microscopy of polymers. *Polym. Sci. Ser. B* **49**, 282–287.

Kramer, E.J. (1979) *Environmental Cracking of Polymers. Developments in Polymer Fracture. Appl. Sci.*, London.

Lagaron, J.M., Dixon, N.M., Reed, W., Pastor, J.M. & Kip, B.J. (1999) Morphological characterisation of the crystalline structure of cold-drawn HDPE used as a model material for the environmental stress cracking (ESC) phenomenon. *Polymer* **40**, 2569–2586.

Lee, S.-Y., Park, S.-Y. & Song, H.-S. (2006) Lamellar crystalline structure of hard elastic HDPE films and its influence on microporous membrane formation. *Polymer* **47**, 3540–3547.

Li, D.S., Garmestani, H., Alamo, R.G. & Kalidindi, S.R. (2003) The role of crystallinity in the crystallographic texture evolution of polyethylenes during tensile deformation. *Polymer* **44**, 5355–5367.

Lu, J., Sue, H.J. & Rieker, T.P. (2001) Dual crystalline texture in HDPE blown films and its implication on mechanical properties. *Polymer* **42**, 4635–4646.

Magonov, S.N. & Reneker, D.H. (1997) Characterization of polymer surfaces with atomic force microscopy. *Ann. Rev. Mater. Sci.* **27**, 175–222.

Magonov, S. & Yerina, N. (2005) Visualization of nanostructures with atomic force microscopy. *Handbook of Microscopy for Nanotechnology* (eds. by N. Yao & Z. Wang). pp. 113–155. Springer, New York.

Oderkerk, J., de Schaetzen, G., Goderis, B., Hellemans, L. & Groeninckx, G. (2002) Micromechanical deformation and recovery processes of nylon-6/rubber thermoplastic vulcanizates as studied by atomic force microscopy and transmission electron microscopy. *Macromolecules* **35**, 6623–6629.

Opdahl, A. & Somorjai, G.A. (2001) Stretched polymer surfaces: atomic force microscopy measurement of the surface deformation and surface elastic properties of stretched polyethylene. *J. Polym. Sci. B Polym. Phys.* **39**, 2263–2274.

Petermann, J., Gohil, R.M., Massud, M. & Göritz, D. (1982) Plastic deformation of linear polyethylene containing row structures. *J. Mater. Sci.* **17**, 100–104.

Plummer, C.J.G., Goldberg, A. & Ghanem, A. (2001) Micromechanisms of slow crack growth in polyethylene under constant tensile loading. *Polymer* **42**, 9551–9564.

Prasad, A., Shroff, R., Rane, S. & Beaucage, G. (2001) Morphological study of HDPE blown films by SAXS, SEM and TEM: a relationship between the melt elasticity parameter and lamellae orientation. *Polymer* **42**, 3103–3113.

Robeson, L.M. (2013) Environmental stress cracking: a review. *Polym. Eng. Sci.* **53**, 453–467.

Rukhlya, E.G., Litmanovich, E.A., Dolinnyi, A.I., Yarysheva, L.M., Volynskii, A.L. & Bakeev, N.F. (2011) Penetration of poly(ethylene oxide) into the nanoporous structure of the solvent-crazed poly(ethylene terephthalate) films. *Macromolecules* **44**, 5262–5267.

Sinevich, E.A., Bykova, I.V. & Bakeev, N.F. (1998) Effect of the interphase surface energy on the structure of crazed polymers. *Polym. Sci. Ser. B* **40**, 327–335.

Sprague, B.S. (1973) Relationship of structure and morphology to properties of "hard" elastic fibers and films. *J. Macromol. Sci. Part B* **8**, 157–187.

Thomas, C., Ferreiro, V., Coulon, G. & Seguela, R. (2007) In situ AFM investigation of crazing in polybutene spherulites under tensile drawing. *Polymer* **48**, 6041–6048.

Thomas, C., Seguela, R., Detrez, F., Miri, V. & Vanmansart, C. (2009) Plastic deformation of spherulitic semi-crystalline polymers: an in situ AFM study of polybutene under tensile drawing. *Polymer* **50**, 3714–3723.

Trofimchuk, E.S., Nesterova, E.A., Meshkov, I.B., Nikonorova, N.I., Muzafarov, A.M. & Bakeev, N.P. (2007) Polypropylene/silicate composites on the basis of crazed polymer and hyperbranched polyethoxysiloxane. *Macromolecules* **40**, 9111–9115.

Trofimchuk, E.S., Nikonorova, N.I., Chagarovskii, A.O., Volynskii, A.L. & Bakeev, N.F. (2005a) Crystallization of silver chloride in crazed porous polymers. *J. Phys. Chem. B* **109**, 16278–16283.

Trofimchuk, E.S., Nikonorova, N.I., Dedushenko, S.K. & Perfiliev, Y.D. (2005b) Mössbauer investigation of highly dispersed iron particles in crazed porous polymers. *HFI/NQI 2004* (eds. by K. Maier & R. Vianden). pp. 81–86. Springer, Berlin, Heidelberg.

Trofimchuk, E.S. & Yablokova, M.Y. (2001) Calculation of the basic kinetic parameters of thermo-oxidative degradation of polyethylene and its copper-containing composites. *Polym. Degrad. Stability* **74**, 291–295.

Volynskii, A.L., Arzhakova, O.V., Yarysheva, L.M. & Bakeev, N.F. (2000) Delocalized solvent crazing of polymers. *Polym. Sci. Ser. B* **42**, 549–564.

Volynskii, A.L., Yarysheva, A.Yu., Rukhlya, E.G., Efimov, A.V., Yarysheva L.M. & Bakeev, N.F. (2013) Strain-induced softening of glassy and crystalline polymers. *Russ. Chem. Rev.* **82**, 988–1006.

Volynskii, A.L. & Bakeev, N.F. (1995) *Solvent Crazing of Polymers*. Elsevier, Amsterdam, New York.

Volynskii, A.L. & Bakeev, N.F. (2009) Healing of interfacial surfaces in polymer systems. *Polym. Sci. Ser. A* **51**, 1096–1126.

Wawkuschewski, A., Cantow, H.J., Magonov, S.N., Sheiko, S.S. & Möller, M. (1993) Scanning force microscopy of nanofibrillar structure of drawn polyethylene tapes. *Polym. Bull.* **31**, 699–705.

Yang, D.C. & Thomas, E. (1984) An electron microscopy and X-ray diffraction study of the microstructures of melt-drawn polyethylene films. *J. Mater. Sci.* **19**, 2098–2110.

Yarysheva, A.Y., Bagrov, D.V., Rukhlya, E.G., Yarysheva, L.M., Volynskii, A.L. & Bakeev, N.F. (2011) First direct microscopic study of the crazed polymer structure stabilized by a liquid medium. *Doklady Phys. Chem.* **440**, 198–200.

Yarysheva, A., Bagrov, D., Rukhlya, E., Yarysheva, L., Volynskii, A. & Bakeev, N. (2012) Features of the delocalized crazing of high-density polyethylene in poly(ethylene oxide) solutions. *Polym. Sci. Ser. A* **54**, 779–786.

Yarysheva, L.M., Galperina, N.B., Arzhakova, O.V., Volynskii, A.L., Bakeev, N.F. & Kozlov, P.V. (1989) Using of the liquid permeation method to determine the structure of crazes arising under deformation of polymers in liquid-media. *Polym. Sci. Ser. B* **31**, 211–216.

Yefimov, A., Sherba, V., Ozerin, A., Rebrov, A. & Bakeev, N. (1990) Structure of crazes formed as a result of deformation of polyethylene terephthalate at various temperatures. *Polym. Sci. Ser. A* **32**, 828–834.

Yefimov, A., Valiotti, N., Dakin, V., Ozerin, A. & Bakeev, N. (1988) Effect of chemical crosslinking on crazing of polyethylene in liquid-medium. *Polym. Sci. Ser. A* **30**, 963–968.

Zhang, X.M., Elkoun, S., Ajji, A. & Huneault, M.A. (2004) Oriented structure and anisotropy properties of polymer blown films: HDPE, LLDPE and LDPE. *Polymer* **45**, 217–229.